Bioorganic & Medicinal Chemistry Letters 19 (2009) 1991–1995

Contents lists available at ScienceDirect

Bioorganic & Medicinal Chemistry Letters

journal homepage: www.elsevier.com/locate/bmcl

(3,3-Difluoro-pyrrolidin-1-yl)-[(2*S*,4*S*)-(4-(4-pyrimidin-2-yl-piperazin-1-yl)-pyrrolidin-2-yl]-methanone: A potent, selective, orally active dipeptidyl peptidase IV inhibitor

Mark J. Ammirati, Kim M. Andrews, David D. Boyer, Anne M. Brodeur, Dennis E. Danley, Shawn D. Doran, Bernard Hulin, Shenping Liu, R. Kirk McPherson, Stephen J. Orena, Janice C. Parker, Jana Polivkova, Xiayang Qiu, Carolyn B. Soglia, Judith L. Treadway, Maria A. VanVolkenburg, Donald C. Wilder, David W. Piotrowski *

Pfizer Global Research & Development, Groton/New London Laboratories, Pfizer Inc, Groton, CT 06340, United States

ARTICLE INFO

Article history:
Received 1 December 2008
Revised 9 February 2009
Accepted 10 February 2009
Available online 13 February 2009

Keywords:
Dipeptidyl peptidase IV
DPP-4
Diabetes

ABSTRACT

A series of 4-substituted proline amides was synthesized and evaluated as inhibitors of dipeptidyl pepdidase IV for the treatment of type 2 diabetes. (3,3-Difluoro-pyrrolidin-1-yl)-[(2*S*,4*S*)-(4-(4-pyrimidin-2-yl-piperazin-1-yl)-pyrrolidin-2-yl]-methanone (**5**) emerged as a potent (IC_{50} = 13 nM) and selective compound, with high oral bioavailability in preclinical species and low plasma protein binding. Compound **5**, PF-00734200, was selected for development as a potential new treatment for type 2 diabetes.

Type 2 diabetes mellitus is a chronic disorder characterized by hyperglycemia coupled with a gradual decline in insulin sensitivity and insulin secretion. The incretin hormone glucagon-like peptide-1 (GLP-1), which is released post-prandially from the L-cells of the intestine, stimulates the release of insulin from pancreatic β-cells. However, GLP-1 is rapidly degraded in vivo by peptidases, including dipeptidyl peptidase IV (DPP-4), which is a widely distributed serine protease that specifically cleaves N-terminal dipeptides from polypeptides with proline or alanine at the penultimate position. In vivo administration of DPP-4 inhibitors to human subjects results in higher circulating concentrations of endogenous GLP-1 and subsequent decrease in plasma glucose. Long term treatment with a DPP-4 inhibitor leads to a reduction in circulating HbA1c (glycosylated hemoglobin). DPP-4 inhibition also offers the potential to improve the insulin producing function of the pancreas through either β-cell preservation or regeneration. Therefore, DPP-4 inhibition has emerged as a promising new treatment of Type 2 diabetes.[1]

Clinical proof of concept has been established for several DPP-4 clinical candidates, two of which have become marketed drugs. Januvia™ (sitagliptin phosphate, **1**) has recently been approved by the US Food and Drug Administration (FDA) for the treatment of type 2 diabetes and Galvus™ (vildagliptin, **2**) has been approved by the European Medicines Agency. Several other DPP-4 inhibitors are currently being evaluated in human clinical trials including saxagliptin **3**, alogliptin **4** and PF-00734200 **5**.

DPP-4 inhibitors containing electrophiles (nitriles, boronic acids) as part of a proline P1 group are highly potent and display a time-dependent kinetic profile. However, a delicate balance between potency and chemical stability is required to achieve suitable drug-like attributes.[2] Competitive inhibitors, such as the highly ligand efficient[3] thiazolidide P32/98 **6**, can exhibit better chemical stability. While substrate analog **6** is among the smallest known P2-P1 fragments,[4] thiazolidine amides can elicit profound toxicological effects.[5] Reports from Pfizer and other laboratories have demonstrated that fluorinated azetidines and pyrrolidines can not only function as P1 binding fragments but can also offer potency gains relative to their non-fluorinated counterparts.[6] It has also been established that some additional potency gains can be achieved by maximizing interactions of the P2 fragment.[7] Our ideal candidate would possess reversible, competitive enzyme kinetics, achieve rapid onset of action, and be administered in a low-dose consistent with once-a-day dosing. These requirements stipulate that the compound not only be highly potent but also

* Corresponding author. Tel.: +1 860 686 0271; fax: +1 860 686 6627.
E-mail address: david.w.piotrowski@pfizer.com (D.W. Piotrowski).

0960-894X/$ - see front matter © 2009 Elsevier Ltd. All rights reserved.
doi:10.1016/j.bmcl.2009.02.041

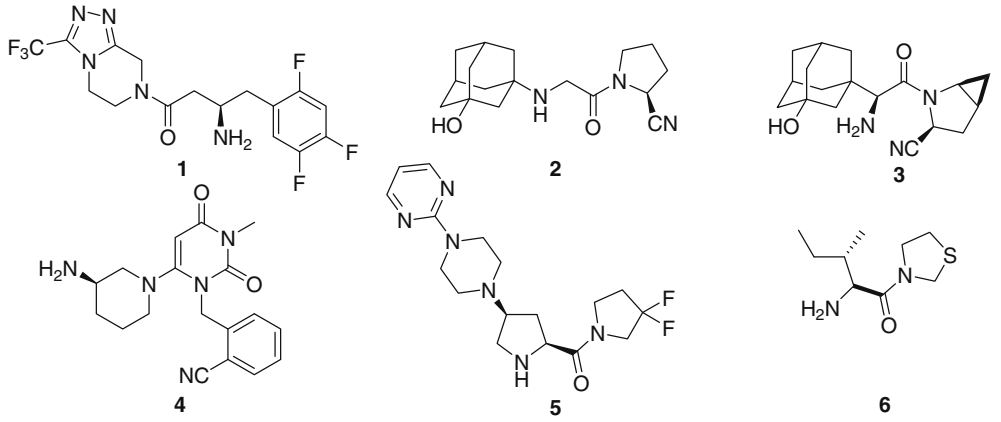

possess high permeability, low intrinsic clearance and high solubility.

The natural constraint provided by a prolyl pyrrolidide P2-P1 fragment offered an ideal scaffold to explore both the P1 and P2 portions of the molecule. The P1 fragment was explored by incorporation of fluorinated amines[6a] by a standard amide bond coupling to the commercially available *N*-BOC-L-ketoproline **7**. The P2 portion of the scaffold was explored by reductive amination of ketone **8** with a range of substituted piperidines, pyrrolidines, piperazines, homopiperazines and heterocyclic fused variants thereof. The heterocyclic substituted piperazines offered the best balance of potency and selectivity for the increase in molecular weight. Specifically, the hydrochloride salts of **5**, **9–25** were accessed by substrate controlled, stereoselective reductive amination followed by BOC deprotection according to Scheme 1. In general, the reductive amination step afforded only the cis isomer. The stereochemistry of **5** was confirmed as cis (2*S*,4*S*) by single crystal X-ray crystallography.[8] The trans isomer **26** was prepared by reduction of ketone **8**, in situ formation of the triflate followed by displacement with 2-pyrimidinylpiperazine and BOC deprotection.

A combination of DPP-4 potency and selectivity against DPP-8 was used to advance compounds, with the minimum criteria for further consideration being DPP-4 IC_{50} less than 20 nM and greater than 100-fold selectivity versus DPP-8. Table 1 summarizes the inhibitory properties for selected analogs.[9a,c,10] The cis isomer **5** was ~24× more potent than the trans isomer **26**. Compounds with the unnatural proline 2R-stereochemistry (data not shown) were inactive at the highest concentration tested (3 μM). Thus, we focused on compounds with 2*S*,4*S* stereochemistry. Mono- or bicyclic analogs **5**, **9**–**16** all displayed high potency and a varying degree of selectivity over DPP-2 and DPP-8. Bicyclic analogs like **11**, **12** and **16** were generally more DPP-2 selective, while monocyclic analogs **5** and **15** showed higher selectivity over DPP-8. Pyrimidine **5** displayed a balance of potency, selectivity, ADME and physical properties. Thus, exploration of the amide portion was done while holding the 2-pyrimidinylpiperazine constant. Amides **18–22** and **24–25** were derived from fluorinated pyrrolidines and azetidines. The general amide SAR trend was pyrrolidide > azetidide >> piperidide (data not shown), with certain fluorinated versions thereof being more potent than their non-fluorinated analogs. Removal, addition or transposition of fluorine atoms relative to **5**, as shown in examples **17–19**, **21** and **22**, led to reduced potency. Of note were meso-difluoropyrrolidide **20** and fluoroazetidide **24**, which were potent and offered high selectivity over both DPP-2 and DPP-8.

The co-crystal structure of compound **5** in recombinant human DPP-4 confirmed the expected binding mode in the active site of DPP-4. The difluoropyrrolidide moiety has extensive hydrophobic

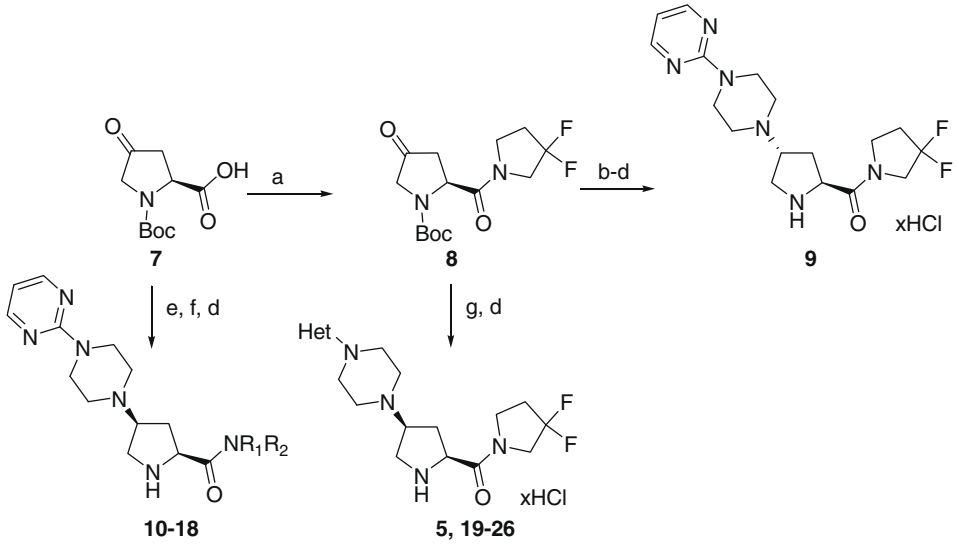

Scheme 1. Reagents and conditions: (a) 3,3-difluoropyrrolidine hydrochloride, EDC, HOBt, TEA, DCM, rt; (b) $NaBH_4$, MeOH, (c) (1) trifluoromethane-sulphonyl chloride, DIPEA, DCM; (2) 2-(1-piperazinyl)pyrimidine, DCM, −10 °C; (d) 4 N HCl in dioxane, rt; (e) 2-(1-piperazinyl)pyrimidine, $NaBH(OAc)_3$, AcOH, DCE; (f) R_1R_2NH hydrochloride, EDC, HOBt TEA, DCM, 0–rt; (g) N-heterocyclic piperazine, $NaBH(OAc)_3$, AcOH, DCE.

Table 1
Human DPP inhibition, ADME and physicochemical properties of N-heterocyclicpiperazinylproline amides

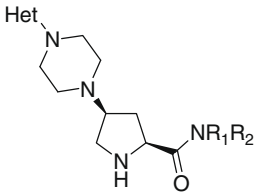

Compd	Het	NR_1R_2	DPP-4 IC_{50}, nM[a]	DPP-2 IC_{50}, μM[a]	DPP-8 IC_{50}, μM[a]	cELog*D*[b]	MDCK[c] (AB/BA)	DOF[d]% inh @10 μM	hERG[e] IC_{50}, μM
5	2-Pyrimidinyl	3,3-Difluoropyrrolidine	12.9 ± 4.6	3.3 ± 0.6	7.0 ± 0.5	0.61	13.0/11.0	14.9	126
9	3-Benzisoxazolyl	3,3-Difluoropyrrolidine	8.7	1.23	2.24	2.12	18.6/11.2	26.7	
10	2-Benzoxazolyl	3,3-Difluoropyrrolidine	8.2	2.26	2.66	1.84	nd	nd	
11	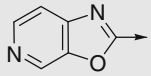	3,3-Difluoropyrrolidine	7.4	7.12	0.97	1.08	nd	nd	
12	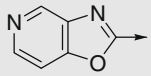	3,3-Difluoropyrrolidine	5.8	8.47	1.15	1.23	nd	8.1	
13	2-Pyrazinyl	3,3-Difluoropyrrolidine	5.6	0.66	0.54	0.61	9.4/10.4	5.4	
14	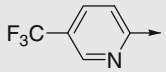	3,3-Difluoropyrrolidine	5.2	0.66	0.53	2.11	16.3/11.4	80.2	40.3% at 0.3 μM
15	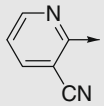	3,3-Difluoropyrrolidine	4.8	0.21	9.15	0.93	10.4/13.5	−7.3	>10
16	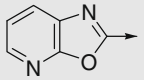	3,3-Difluoropyrrolidine	5.2 ± 3.3	2.88	2.39	1.48	nd	7.4	
17	2-Pyrimidinyl	Pyrrolidine	31	20.4	9.69	−0.11	5.7/7.4	18.0	
18	2-Pyrimidinyl	(*R*)-3-Fluoropyrrolidine	51	28.3	10.3	0.28	11.6/7.0	2.7	
19	2-Pyrimidinyl	(*S*)-3-Fluoropyrrolidine	31	31.4	15.1	0.28	8.5/6.0	6.4	
20	2-Pyrimidinyl	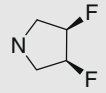	13	11.1	17.1	0.44	3.7/6.7	7.2	54
21	2-Pyrimidinyl	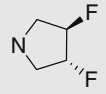	309	nd	nd	0.44	15.6/9.4	−1.6	
22	2-Pyrimidinyl		25	2.46	7.88	1.43	23.0/11.5	1.0	
23	2-Pyrimidinyl	Azetidine	309	nd	nd	−0.28	2.7/2.4	−6.0	
24	2-Pyrimidinyl	3-Fluoroazetidine	41	>30	>30	−0.06	12.8/6.4	−1.5	
25	2-Pyrimidinyl	3,3-Difluoroazetidine	134	nd	nd	0.51	nd	nd	
26[f]	2-Pyrimidinyl	3,3-Difluoropyrrolidine	338	nd	nd		nd	nd	

[a] Recombinant wild-type human enzyme DPP-4,[10a] DPP-2,[9a] DPP-8.[9c] Where available, values are means of two to four experiments. Typical standard deviations are ± 15%.
[b] clog*D* calculated from an in-house rule-based regression model based on experimental Log*D*.
[c] MDCK = Madin Darby Canine Kidney cells, Papp, 10^{-6} cm/s.
[d] DOF = [^{3}H]-dofetilide binding assay.[11a,b]
[e] hERG patch clamp.[11c]
[f] Trans (2S,4R) stereochemistry. nd = not determined.

interactions with the side chains of Trp659, Val 656, Tyr631, Ser630, Tyr666 and Tyr662 that form the S1 pocket. One of the pyrrolidide fluorines appears to be within hydrogen bonding distance to form a hydrogen bond with either the side chain of Ser630 or the main chain amide of Tyr631. The secondary amine of the pyrrolidine forms a salt bridge with the conserved glutamate cluster, Glu206 and Glu205. The pyrimidine extends to Phe357 and forms a pi–pi stacking interaction with its side chain (Fig. 1).[12]

Desirable safety properties, in particular hERG, could be adjusted by careful control of Log*D*. For this series, there was a strong correlation between Log*D* and percent inhibition [^{3}H]-dofetilide binding at 10 μM, where Log*D* > 1.5 increased the probability of high percent dofetilide inhibition. High percent inhibition in the dofetilide assay corresponded to high affinity for the hERG channel as measured in patch clamp experiments.[11d] For example, **14** had a high percent inhibition in the dofetilide binding assay and high affinity for hERG while **5**, **15** and **20** had a low percent inhibition

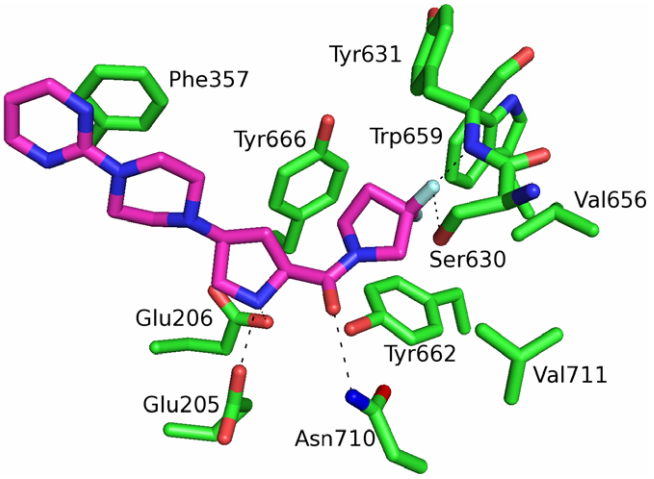

Figure 1. Binding interactions in the active site. Compound **5** co-crystallized with human DPP-4.

and low affinity for the hERG channel. Thus, low hERG and high potency/selectivity space could be defined as 0.5 > Log *D* < 1.5. ADME properties such as in vitro microsomal stability and high flux in permeability assays could be obtained by working within this physicochemical property space.

Compounds **5**, **15**, **20** and **24** were selected for in vivo evaluation based on their in vitro profiles: pharmacokinetic (PK) data are summarized in Table 2. Compound **17** was included as a non-fluorinated comparator. Compounds **5**, **20** and **24** all exhibited moderate clearance, moderate volume of distribution, moderate half life and good bioavailability, while **15** was characterized by a high clearance and low bioavailability. Compound **5** achieved and maintained higher plasma concentrations than did the non-fluorinated comparator **17**, which had a clearance higher than rat liver blood flow. Based on the desirable PK properties in rat, **5** was advanced to further PK profiling in dog and monkey, where moderate clearance, moderate volume of distribution, moderate half-life and good bioavailability were again noted. The low turnover from in vitro systems (microsomes and hepatocytes[13]) suggested that cytochrome P450 mediated metabolism was not a major clearance mechanism for compound **5**. In vivo data from the rat, dog and monkey supported this conclusion, since, even with moderate clearance the bioavailability across species was high suggesting that first-pass metabolism was minimal. Human clearance was predicted using allometric scaling of rat, dog and monkey clearance data (Table 3).

Compound **5** was further assessed in an advanced battery of in vitro assays, for which the data are summarized in Table 3. Of note was the high selectivity over closely related serine proteases and P450 enzymes as well as selectivity over a wide panel of enzymes, receptors and ion channels. No notable binding differences

Table 3
Pharmacological and ADME properties of **5**

		5
Human plasma DPP-4 IC_{50}		11.3 ± 2.7 nM[a]
Rat plasma DPP-4 IC_{50}		12.8 nM
Selectivity[b]		>400×
DPP-3	>30,000 nM	
DPP-9	5980 nM	
APP	>30,000 nM	
FAP	10,300 nM	
POP	>30,000 nM	
Projected human CL[c]		2.6 mL/min/kg
Projected human Vd[d]		1.0 L/kg
Projected F%[e]		70
CEREP broad receptor and enzyme profile (73 assays)		IC_{50} > 10 μM
CYP1A2, 2C9, 2C19, 2D6, 3A4		IC_{50} > 30 μM

[a] Values are means of at least three experiments.
[b] DPP-3, DPP-9, APP, FAP, POP.[9]
[c] Projected value based on allometry (total).
[d] Projected by multiple methods (allometry, Oie-Tozer and dog-human proportionality).
[e] Projected value based on preclinical F%.

were observed between rat and human plasma DPP-4 enzyme. On the basis of desirable drug-like properties, excellent PK properties and synthetic simplicity, **5** was selected for in vivo profiling. An ex vivo plasma DPP-4 inhibition assay utilizing 50 μM substrate (GlyProAMC) and corrected for plasma dilution was used to assess the pharmacodynamic profile.[10] Maximal efficacy (E_{max}) and IC_{50} were determined to be 98% and 1.3 ng/mL, respectively, (Fig. 2). Because **5** exhibited a high free fraction (80–100%) in rat, dog, monkey and human, the human dose projection could be set using the rat PK–PD relationship and the human DPP-4 inhibition data without correction. Thus, administration of single oral doses of **5**

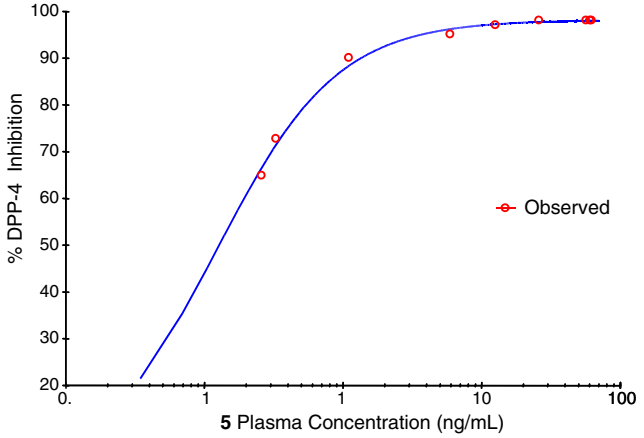

Figure 2. PK–PD in Sprague–Dawley rats using an ex-vivo plasma DPP-4 inhibition assay.

Table 2
Pharmacokinetic profiles of selected DPP-4 inhibitors[a]

Cmpd	Species	CL_p (mL/min/kg)	Vss (L/kg)	$t_{1/2}$ (h)	F (%)	po AUC (ng h/mL)	po C_{max} (ng/mL)
5	Rat	38	1.9	2.5	109	2398	1406
	Dog	3.7	0.7	2.9	95	7162	1526
	Monkey	7.6	1.0	7.6	71	843	517
15	Rat	61	1.8	1.5	20	276	237
17	Rat	84	2.5	2.2	78	775	449
20	Rat	27	1.9	2.3	93	3948	1817
24	Rat	16	0.9	3.6	91	1073	1718

[a] Dose: Sprague–Dawley rat, beagle dog, cynomolgus monkey iv: 1 mg/kg in sterile saline; rat po: 5 mg/kg in 0.5% methylcellulose; dog, monkey po: 1 mg/kg in sterile water.

to healthy adult subjects under fasted conditions resulted in mean serum concentrations that increased in a dose proportional manner with ascending doses. Compound **5** was rapidly absorbed with a median T_{max} of 0.5–1.5 h and the estimated mean terminal half-life ranged from 15.1–27.4 h across dose levels of 0.3–300 mg. The mean C_{max} and AUC_{last} increased in an approximately dose-proportional fashion.[14]

In summary, a series of 4-substituted proline amides were evaluated as inhibitors of DPP-4. A potent and selective compound with low clearance, high permeability and low probability for hERG liability was achieved by operating in optimal physicochemical property space. PF-00734200 (**5**), (3,3-difluoro-pyrrolidin-1-yl)-[(2*S*,4*S*)-(4-(4-pyrimidin-2-yl-piperazin-1-yl)-pyrrolidin-2-yl]-methanone, was selected for clinical development. In Phase 1 human trials, PF-00734200 was rapidly absorbed, showed dose-proportional increase in exposure and demonstrated a human PK-PD profile that should permit a once-daily dosing regimen.

Acknowledgments

The authors thank Dr. Greg Berger for support and guidance and Drs. Stephen Wright, John Benbow, David Hepworth and David Price for review of the manuscript. Jon Bordner is thanked for the small molecule X-ray crystal structure determination of compound **5**. Bernard Fermini and Shuya Wang are thanked the for hERG patch clamp studies.

Supplementary data

Supplementary data associated with this article can be found, in the online version, at doi:10.1016/j.bmcl.2009.02.041.

References and notes

1. For comprehensive reviews on DPP-4 inhibitors, see: (a) Idris, I.; Donnelly, R. *Diabetes Obes. Metab.* **2007**, *9*, 153; (b) von Geldern, T. W.; Trevillyan, J. M. *Drug Dev. Res.* **2006**, *67*, 627; (c) Weber, A. E. *J. Med. Chem.* **2004**, *47*, 4135.
2. Peters, J.-U. *Curr. Top. Med. Chem.* **2007**, *7*, 579.
3. Hopkins, A. L.; Groom, C. R.; Alex, A. *Drug Discov. Today* **2004**, *9*, 430.
4. Pospisilik, J. A.; Stafford, S. G.; Demuth, H-U.; Brownsey, R.; Parkhouse, W.; Finegood, D. T.; McIntosh, C. H. S.; Pederson, R. A. *Diabetes* **2002**, *51*, 943.
5. For a discussion of toxicities associated with thiazolidides like P32/98, see: Thornberry, N. A.; Weber, A. E. *Curr. Top. Med. Chem.* **2007**, *7*, 557.
6. (a) Hulin, B.; Cabral, S.; Lopaze, M. G.; Van Volkenberg, M. A.; Andrews, K. M.; Parker, J. C. *Bioorg. Med. Chem. Lett.* **2005**, *15*, 4770; (b) Edmondson, S. D.; Mastracchio, A.; Mathvink, R. J.; He, J.; Harper, B.; Park, Y.-J.; Beconi, M.; Di Salvo, J.; Eiermann, G. J.; He, H.; Leiting, B.; Leone, J. F.; Levorse, D. A.; Lyons, K.; Patel, R. A.; Patel, S. B.; Petrov, A.; Scapin, G.; Shang, J.; Roy, R. S.; Smith, A.; Wu, J. K.; Xu, S.; Zhu, B.; Thornberry, N. A.; Weber, A. E. *J. Med. Chem.* **2006**, *49*, 3614.
7. Yoshida, T.; Sakashita, H.; Akahoshi, F.; Hayashi, Y. *Bioorg. Med. Chem. Lett.* **2007**, *17*, 2618. and refereneces cited therein.
8. An ORTEP plot and atomic coordinates for **5** are included in the Supplementary data associated with this article. Additional analytical data for the free base of **5**: mp 156 °C; MS (AP) *m/z* 367.4 (M^+); ^1H NMR (400 MHz, D_2O): δ 8.15 (d, 2H, *J* = 5.0 Hz, *CH* of pyrimidine), 6.55 (t, 1H, *J* = 4.8 Hz, *CH* of pyrimidine), 3.87–3.81 (dd, 1H, H_{2b} of proline, rotomeric), 3.78–3.50 (m, 4H, N–CH_2 of pyrrolidide), 3.55–3.40 (m, 4H, N–CH_2 of piperazine), 2.97 (dd, 1H, *J* = 10.2, 6.6 Hz, H_{5a} of proline), 2.85–2.75 (m, 1H, H_{4b} of proline), 2.69 (dd, 1H, *J* = 10.0, 9.1 Hz, H_{5b} of proline), 2.55–2.20 (m, 7H, overlapping N–CH_2 of piperazine, CH_2 of pyrrolidide and H_{3b} of proline), 1.47–1.38 (m, 1H, H_{3a} of proline); Anal. Calcd for $C_{17}H_{24}F_2N_6O$: C, 55.73; H, 6.60; N, 22.94. Found: C, 55.78; H, 6.54; N, 22.68.
9. DPP-2 substrate 200 μM Lys-Ala-β-naphthylamide. See: (a) McDonald, J. K.; Leibach, F. H.; Grindeland, R. E.; Ellis, S. *J. Biol. Chem.* **1968**, *243*, 4143–4150; DPP-3 substrate 125 μM Arg-Arg-AMC. See: (b) Abramic, M.; Zubanovic, M.; Vitale, L. *Biol. Chem.* **1988**, *369*, 29–38; DPP-8 substrate 200 μM Ala-Pro-AMC. See: (c) Abbot, C. A.; Yu, D. M.; Woollatt, E.; Sutherland, G. R.; McCaughan, G. W.; Gorrell, M. D. *Eur. J. Biochem.* **2000**, *267*, 6140–6150; DPP-9 substrate 200 μM Ala-Pro-AMC. See: (d) Olsen, C.; Wagtmann, N. *Gene* **2002**, *299*, 185–193; FAP substrate 200 μM Ala-Pro-AMC. See: (e) Scanlan, M. J.; Raj, B. K. M.; Calvo, B.; Garin-Chesa, P.; Sanz-Moncasi, M. P.; Healey, J. H.; Old, L. J.; Rettig, W. J. *Proc. Natl. Acad. Sci. U.S.A.* **1994**, *91*, 5657–5661; APP substrate 500 μM Arg-Pro-Pro. See: (f) Rusu, I.; Yaron, A. *Eur. J. Biochem.* **1992**, *210*, 93–100; POP substrate 200 μM Z-Gly-Pro-AMC. See: (g) Yoshimoto, T.; Orlowski, R. C.; Walter, R. *Biochemistry* **1977**, *16*, 2942.
10. The dipeptidyl peptidase enzyme inhibition assays and rat pharmacokinetic assays are described in: (a) Wright, S. W.; Ammirati, M. J.; Andrews, K. M.; Brodeur, A. M.; Danley, D. E.; Doran, S. D.; Lillquist, J. S.; McClure, L. D.; McPherson, R. K.; Orena, S. J.; Parker, J. C.; Polivkova, J.; Qiu, X.; Soeller, W. C.; Soglia, C. B.; Treadway, J. L.; VanVolkenberg, M. A.; Wang, H.; Wilder, D. C.; Olson, T. V. *J. Med. Chem.* **2006**, *49*, 3068; The pharmacodynamic assay is described in: (b) Kim, D.; Wang, L.; Beconi, M.; Eiermann, G. J.; Fisher, M. H.; He, H.; Hickey, G. J.; Kowalchick, J. E.; Leiting, B.; Lyons, K.; Marsilio, F.; McCann, M. E.; Patel, R. A.; Petrov, A.; Scapin, G.; Patel, S. B.; Sinha Roy, R.; Wu, J. K.; Wyvratt, M. J.; Zhang, B. B.; Zhu, L.; Thornberry, N. A.; Weber, A. E. *J. Med. Chem.* **2005**, *48*, 141.
11. (a) *Affinity-Assay for the Human ERG Potassium Channel*; Greengrass, P. M.; Stewart, M.; Wood, C. M. PCT Patent Application WO 03/021271.; (b) Singleton, D. H.; Boyd, H.; Steidl-Nichols, J. V.; Deacon, M.; de Groot, M. J.; Price, D.; Nettleton, D. O.; Wallace, N. K.; Troutman, M. D.; Williams, C.; Boyd, J. G. *J. Med. Chem.* **2007**, *50*, 2931; (c) Hamill, O. P.; Marty, A.; Neher, E.; Sakmann, B.; Sigworth, F. J. *Eur. J. Physiol.* **1981**, *391*, 85–100; (d) Diaz, G. J.; Daniell, K.; Leitza, S. T.; Martin, R. L.; Su, Z.; McDermott, J. S.; Cox, B. F.; Gintant, G. A. *J. Pharmacol. Toxicol. Methods* **2004**, *50*, 187.
12. The structure has been deposited in the Protein Data Bank with the deposition code 3F8S.
13. In vitro clearance values for compound **5**: Human liver microsome intrinsic clearance (HLM CLint) < 7.0 mg/mL/kg, *n* = 4. Human hepatocyte intrinsic clearance (HH Clint) < 7.1 mg/mL/kg, *n* = 2.
14. Dai, H.; Gustavson, S. M.; Preston, G. M.; Eskra, J. D.; Calle, R.; Hirshberg, B. *Diabetes Obes. Metab.* **2008**, *10*, 506.